Published in final edited form as:

Circulation. 2020 October 27; 142(17): 1667–1683. doi:10.1161/CIRCULATIONAHA.120.045470.

4HNE Impairs Myocardial Bioenergetics in Congenital Heart Disease-induced Right Ventricular Failure

HyunTae V Hwang, PhD[1], **Nefthi Sandeep, MD**[1], **Sharon L. Paige, MD, PhD**[1], **Sara Ranjbarvaziri, PhD**[1], **Dong-Qing Hu, MD**[1], **Mingming Zhao, MD**[1], **Ingrid S. Lan, MS**[2], **Michael Coronado, PhD**[3], **Kristina B. Kooiker, PhD**[4], **Sean M. Wu, MD, PhD**[5], **Giovanni Fajardo, MD**[1], **Daniel Bernstein, MD**[1], **Sushma Reddy, MD**[1]

[1]Department of Pediatrics (Cardiology), Stanford University, Palo Alto, CA

[2]Department of Bioengineering, Stanford University, Palo Alto, CA

[3]Department of Biology, Whitman College, Walla Walla, WA

[4]Department of Medicine, University of Washington, Seattle, WA

[5]Department of Medicine (Cardiology), Stanford University, Palo Alto, CA;

Abstract

Background: In patients with complex congenital heart disease, such as those with tetralogy of Fallot, the right ventricle (RV) is subject to pressure overload stress, leading to RV hypertrophy and eventually RV failure. The role of lipid peroxidation, a potent form of oxidative stress, in mediating RV hypertrophy and failure in congenital heart disease is unknown.

Methods: Lipid peroxidation and mitochondrial function and structure were assessed in RV myocardium collected from patients with RV hypertrophy with normal RV systolic function (RV FAC 47.3±3.8%) and in patients with RV failure showing decreased RV systolic function (RV FAC 26.6±3.1%). The mechanism of the effect of lipid peroxidation, mediated by 4-hydroxynonenal (4HNE; a byproduct of lipid peroxidation) on mitochondrial function and structure was assessed in HL1 murine cardiomyocytes and human induced pluripotent stem cell-derived cardiomyocytes.

Results: RV failure was characterized by an increase in 4HNE adduction of metabolic and mitochondrial proteins (16/27 identified proteins), in particular electron transport chain proteins. Sarcomeric (myosin) and cytoskeletal proteins (desmin, tubulin) also underwent 4HNE-adduction. RV failure showed lower oxidative phosphorylation [moderate RV hypertrophy 287.6±19.75 vs. RV failure 137.8±11.57 pmol/(sec*ml), p=0.0004], and mitochondrial structural damage. Using a cell model, we show that 4HNE decreases cell number and oxidative phosphorylation (control 388.1±23.54 vs. 4HNE 143.7±11.64 pmol/(sec*ml), p<0.0001). Carvedilol, a known antioxidant did not decrease 4HNE adduction of metabolic and mitochondrial proteins and did not improve oxidative phosphorylation.

Corresponding Author: Sushma Reddy, 750 Welch Rd, Suite 305, Stanford University, Palo Alto, CA 94305-5731. Fax No: (650) 725-8343; Telephone No: (650) 736-8752; sureddy@stanford.edu.

Disclosures: The authors have declared that no conflict of interest exists.

Conclusions: Metabolic, mitochondrial, sarcomeric and cytoskeletal proteins are susceptible to 4HNE-adduction in patients with RV failure. 4HNE decreases mitochondrial oxygen consumption by inhibiting electron transport chain complexes. Carvedilol did not improve the 4HNE-mediated decrease in oxygen consumption. Strategies to decrease lipid peroxidation could improve mitochondrial energy generation and cardiomyocyte survival and improve RV failure in patients with congenital heart disease.

Keywords

Right ventricle; congenital heart disease; hypertrophy; heart failure; mitochondria; lipid peroxidation

Introduction

Children with complex congenital heart disease involving right-sided obstructive lesions such as tetralogy of Fallot, pulmonary atresia/intact ventricular septum, and hypoplastic left heart syndrome or pulmonary hypertension are at risk for right ventricular (RV) failure and decreased survival[1–3]. However, the incidence and timing of RV failure varies[2, 4], and current non-invasive and invasive diagnostic modalities can neither predict which patients will progress to RV failure nor detect the preceding subclinical changes occurring on the molecular and cellular level. In addition, standard heart failure therapies such as angiotensin-converting enzyme inhibitors and β blockers are ineffective in the treatment of RV failure[5].

We focused on the critical role of oxidative stress on mitochondrial bioenergetics during RV hypertrophy and the progression to RV failure in congenital heart disease involving right-sided obstructive lesions. The human heart is a highly oxidative organ cycling a daily amount of adenosine triphosphate (ATP) up to 15 to 20 times its own weight[6], and is thus particularly vulnerable to oxidative damage. Oxidation of membrane phospholipids, known as lipid peroxidation, is the most prominent manifestation of oxidative stress in the heart in aging and in ischemia/reperfusion injury, and is uniformly detrimental to cardiac function[7–9]. However, little is known about the role of lipid peroxidation and individual lipid peroxidation products such as the potent reactive aldehyde 4-hydroxynonenal (4HNE) in RV hypertrophy and failure. 4HNE is of particular interest due to its ability to adduct or modify proteins by covalent bonding, thereby inhibiting or altering their function[10, 11]. Since mitochondria are the largest source and target of lipid peroxidation[12], we hypothesized that 4HNE adversely affects mitochondrial energy generation in RV pressure overload, leading to impaired cardiac function and RV failure. Carvedilol, a known antioxidant, has been shown to decrease lipid peroxidation of mitochondrial membranes in ischemic heart disease[13] and to decrease 4HNE expression in dilated cardiomyopathy[14] and was therefore investigated as a candidate drug to rescue lipid peroxidation-induced mitochondrial dysfunction. An improved understanding of the effect of lipid peroxidation on the complex processes of oxidative stress and mitochondrial function could aid in developing novel diagnostic tools for monitoring the progression of the vulnerable RV to failure and for therapeutics to delay the onset of RV failure and improve the quality of life in patients with congenital heart disease.

Methods

The data that support the findings of this study are available from the corresponding author upon reasonable request.

RV myocardial samples from patients with right ventricular outflow tract obstruction

RV muscle bundles routinely resected at the time of cardiac surgery were collected from 16 patients with RV pressure overload due to pulmonary stenosis, double chambered RV or tetralogy of Fallot. Patients were divided into three groups based on qualitative echocardiographic assessment of the degree of hypertrophy by the reading cardiologist: (i) “Mild RV hypertrophy” (N=3), (ii) “Moderate RV hypertrophy” (N=10) and (iii) “Severe RV hypertrophy” (N=3). All patients had RV outflow tract gradients greater than 55 mmHg. RV systolic function measured by RV fractional area change (RV FAC) was normal in all 16 patients. These groups were compared with RV samples from 5 patients with RV pressure overload with pulmonary hypertension secondary to congenital heart disease (repaired atrioventricular septal defect, N=4; Shone’s complex, N=1). These patients had clinical and echocardiographic evidence of RV failure with decreased RV FAC (Table 1), necessitating heart transplantation. It was not possible to obtain healthy, non-hypertrophied RV tissue. RV muscle bundles from mild, moderate and severe RV hypertrophy being resected by the surgeon during cardiac surgery were collected immediately upon resection by the investigator’s team who is on standby in the operating room. For RV failure patients, RV myocardium was resected as soon as the heart was explanted from the patient. 5mg of this freshly resected RV tissue was minced and oxygen consumption was assessed immediately. Biochemical assays and electron microscopy were also evaluated based on sample availability.

Cell culture

HL1 murine cardiomyocytes were cultured in a humidified 5% CO_2, 37°C incubator with complete Claycomb medium (51800C; Sigma-Aldrich; St. Louis, MO), following the manufacturer’s guideline: 10% FBS, 2 mM GlutaMAX™ (35–050-061; ThermoFisher Scientific; Waltham, MA), 100 μM norepinephrine (A0937; Sigma-Aldrich), 300 nM ascorbic acid (A7506; Sigma-Aldrich), and 100 U/ml penicillin-streptomycin (P4333; Sigma-Aldrich).

Protein expression

Standard western blot techniques for denatured and reduced samples were used. The samples were probed using the following antibodies: 4HNE, VDAC1 (voltage-dependent anion-selective channel protein 1), PGC1α (PPARG coactivator 1α), DRP1 (dynamin 1-like), MFF (mitochondrial fission factor), OPA1 (mitochondrial dynamin like GTPase), MFN2 (mitofusin 2), Enolase, and TOM20 (Translocase of outer mitochondrial membrane 20). Mitochondrial fraction was isolated from HL1 cells collected by scraping, following the isolation kit’s dounce-based protocol (89874; ThermoFisher Scientific). Enolase was used as the loading control for total protein and TOM20 for the mitochondrial fraction. Purity of the isolated mitochondria was assessed by confirming the absence of enolase in the mitochondrial fraction (Supplemental Fig Ia). We also confirmed complete removal and

collection of mitochondria from the cytosolic fraction by probing for VDAC1 (Supplemental Fig Ib). Details of the antibodies used are shown in Supplemental Table I.

Identification of 4HNE-adducted proteins

4HNE-adducted proteins increased in RV failure were identified by Applied Biomics (Hayward, CA). Briefly, proteins were separated using 2D-gel electrophoresis in representative RV hypertrophy and RV failure patient samples (N=1/group). 4HNE-adduction levels were measured through western blot. The 4HNE-adducted proteins were identified using mass spectrometry (MALDI-TOF). Similarly, 4HNE adducted proteins were identified in HL1 cardiomyocytes treated with 4HNE and with 4HNE+carvedilol and compared with control.

Mitochondrial Respiration

Using a high resolution Oxygraph2K respirometer (Oroboros Instruments; Innsbruck, Austria), we utilized the Chance and Williams protocol to assess oxygen consumption[15] in 5 mg of fresh, finely minced RV tissue. Non-phosphorylating oxygen consumption due to proton leak (leak respiration) was assessed in response to the substrates (i) malate and glutamate to evaluate complex I-NADH dehydrogenase activity, and (ii) succinate to evaluate complex II-succinate dehydrogenase activity. Subsequently, oxidative phosphorylation was assessed in response to the substrate ADP to evaluate Complex V-mediated maximal respiration (state 3 respiration). Oxidative phosphorylation was calculated by subtracting complex I and II-mediated leak respiration from state 3 respiration. Respiratory control ratio (RCR) was calculated by dividing state 3 respiration by complex I and II-mediated leak respiration. Non-phosphorylating State 4 leak respiration was assessed in response to oligomycin, an ATP synthase inhibitor. Uncoupled respiration was assessed in response to FCCP (Carbonyl cyanide-p-trifluoromethoxyphenylhydrazone) to evaluate the maximal electron transport chain activity[16, 17]. Antimycin A was used to abolish electron transport chain activity. The oxygen consumption rates are reported as O_2 flux per volume (pmol/(sec*ml)). Buffer and substrate concentrations are shown in Supplemental Table II. Oxygen consumption was also assessed in HL1 cardiomyocytes (2 million cells at the time of 4HNE treatment). To further verify our results from HL1 cells, we also measured oxygen consumption in human induced pluripotent stem cell-derived cardiomyocytes (hiPSC-CM) using Seahorse Analyzer (see Supplemental Methods).

Our assay buffer was sufficient to allow entry of the mitochondrial substrates into the samples without other permeabilizing reagents such as saponin. This was evidenced by (1) robust oxygen consumption induced by each administered mitochondrial substrate and uncoupling reagent, and (2) similar levels of ADP-stimulated State 3 respiration to those of uncoupled respiration, which is mediated by the cell-permeable chemical FCCP. In contrast, only negligible levels of oxygen consumption were observed when the samples were suspended in PBS instead (data not shown).

Electron microscopy

Transmission electron microscopy (TEM) (JEM 1400; JEOL; Peabody, MA) was used to assess mitochondrial morphology. RV samples were fixed overnight (2% glutaraldehyde, 4%

paraformaldehyde, 0.1 M sodium cacodylate, pH 7.4), treated with 1% osmium tetroxide, 1% and 3.5% uranyl acetate, and 0.2% lead citrate, sectioned and imaged. Intermyofibrillar mitochondrial number, size, morphology, network and cristae density were analyzed by ImageJ (NIH; Bethesda, MD), tracing all complete mitochondrial perimeters in each image. At least 70 mitochondria per sample were assessed by an investigator blinded to the sample identity.

Mitochondrial DNA copy number

Mitochondrial to nuclear DNA copy number ratio was measured in RV myocardial samples. DNA was isolated from RV samples using QIA DNA Micro Kit (56304; Qiagen; Germantown, MD). Real time quantitative PCR was performed using Human Mitochondrial Monitoring Primer Set (7246; Takara Bio; Mountain View, CA) and PowerUp SYBR Green Master mix (A25742; Applied Biosystems; Foster City, CA).

4HNE treatment of cardiomyocytes

HL1 cells were treated for 24 hours with 50 μM of 4HNE (32100; Cayman Chemical; Ann Arbor, MI), with and without 10 μM carvedilol (S1831; Selleckchem; Houston, TX). An appropriate volume of vehicles was used for other groups that were not treated with these chemicals (ethanol for 4HNE and DMSO for carvedilol). Following treatment, the cells were harvested to assess 4HNE adducted proteins (as described above), oxygen consumption, mitochondrial membrane potential (tetramethylrhodamine, methyl ester; T668; ThermoFisher Scientific), fission and fusion protein expression, mitochondrial mass, and mitochondrial morphology by fluorescence imaging (MitoTracker Red CMXRos; M7512; ThermoFisher Scientific) (see Supplemental Methods). All assays were only performed at 50 μM 4HNE since higher doses at 100 μM and 200 μM were lethal to the cells at 24 hours.

Assessment of mitochondrial morphology

Fluorescence micrographs of mitochondria were quantified using FIJI[18] via custom macros. 7 to 15 micrographs were analyzed per group. The micrographs were background-subtracted with rolling-ball radius of 5, followed by 10 pixels, then de-noised via the Despeckle function. At each step, the signals were normalized with the Enhance Contrast function. The processed images were then thresholded to select the mitochondria, which were subsequently analyzed via the Analyze Particle function. Median values for each micrograph were used for statistical analysis.

Statistics

Student’s T-test was used for comparison between two groups. One-way ANOVA with Tukey’s multiple testing correction was used for three or more group comparisons, and two-way ANOVA was used for groups with two independent variables. For non-normal data, Kruskal-Wallis test was used. Correlation was assessed using Pearson’s correlation. We performed multiple regression analysis to assess differences in oxidative phosphorylation between groups after correcting for age. All data are presented as mean±SEM and description of patient cohort is presented as mean±SD. A p-value of ≤0.05 was considered significant.

Study approval

This study was approved by the Stanford University Institutional Review Board. Consent was obtained from all patients and/or their parents; in addition, assent was obtained for those >7 years of age.

Results

Patient characteristics

RV myocardial samples were collected from patients with mild, moderate and severe RV hypertrophy due to pulmonary stenosis, double chambered RV or tetralogy of Fallot and compared with RV myocardial samples from patients with RV failure due to pulmonary hypertension secondary to repaired atrioventricular septal defect and Shone's complex. RV hypertrophy was qualitatively assessed by echocardiography as mild, moderate and severe RV hypertrophy based on ventricular wall thickness. The mean age of the hypertrophy groups was 13.1±6.5 years and RV failure was 10.9±3.1 years. 39% were male in the hypertrophy groups and 60% in RV failure. Peak RV outflow tract gradient was > 55mmHg in the hypertrophy groups and >50mmHg in RV failure. RV systolic function was normal in the RV hypertrophy groups (RV FAC 47.3±3.8%) and decreased in RV failure (RV FAC 26.6±3.1%). Left ventricular ejection fraction was preserved in all groups (Table 1). Patients in all categories of RV hypertrophy were on no cardiac medications while all patients with RV failure were on systemic inotropes in the form of epinephrine, dopamine and/or milrinone infusions.

4HNE, a lipid peroxidation-induced reactive aldehyde, is increased in patients with RV failure

4HNE protein expression was assessed in RV samples collected from patients with mild, moderate, and severe RV hypertrophy and in patients with RV failure. The level of 4HNE protein adducts was increased in RV failure (moderate RV hypertrophy 0.584±0.222 vs. RV failure 1.647±0.17, p=0.0035) (Fig 1a, b).

Metabolic and mitochondrial proteins are highly susceptible to 4HNE-adduction in RV failure

We next assessed the identity of the proteins susceptible to 4HNE-adduction (Fig 1c–f; N=1/group). Twenty-seven 4HNE-adducted proteins which increased in RV failure (≥1.3 fold change) were selected for identification (Table 2). Interestingly, sixteen of the twenty-seven proteins were metabolic pathway proteins and most were directly related to mitochondrial metabolism. Several proteins involved in electron transport chain activity and mitochondrial respiration including NADH dehydrogenase, cytochrome b, and cytochrome c were affected. Other 4HNE-adducted mitochondrial proteins include the mitochondrial elongation factor EF-Tu, which is critical for mitochondrial protein synthesis and thus can directly impact the assembly of mitochondrial components. In addition, mitochondrial proteins involved in survival and stress-response were targeted by 4HNE. Mitochondrial Stress-70 Protein is a chaperone protein, critical for mitochondrial biogenesis and proteostasis, conferring protection against oxidative and other cytotoxic stresses. Manganese Superoxide Dismutase

(SOD2), a well-recognized mitochondrial antioxidant enzyme, converts toxic mitochondrial superoxides into less reactive hydrogen peroxide. Therefore, 4HNE adduction of metabolic and mitochondrial proteins targets electron transport chain proteins, mitochondrial protein synthesis, and pro-survival pathways.

Cardiac structural proteins are highly susceptible to 4HNE-adduction in RV Failure

Major sarcomeric proteins (myosin) mediating cardiac contraction as well as cytoskeletal proteins (desmin/tubulin) connecting neighboring sarcomeres together and connecting the contractile apparatus to the mitochondria were susceptible to 4HNE-adduction (Table 2). Among the most highly 4HNE adducted proteins were (i) myoglobin, which facilitates oxygen diffusion from the capillaries to the mitochondria (3-fold), (ii) cysteine and glycine-rich protein 3 (25.6-fold), a scaffold protein that promotes assembly of complexes along the sarcomere and which acts as a stretch sensor, and (iii) collagen-1(VI) (6-fold), a major structural component of microfibrils known to cause t-tubule remodeling in heart failure.

Oxidative phosphorylation and uncoupled respiration are impaired in patients with severe RV hypertrophy and RV failure

To understand the significance of the increased 4HNE-adduction to metabolic and mitochondrial proteins in RV failure, we evaluated oxygen consumption in patient myocardial tissues as a marker of mitochondrial function (Fig 2a, b). Complex I and II-mediated leak respiration did not change with RV hypertrophy and failure (Fig 2c, d). Both oxidative phosphorylation (Fig 2e) and uncoupled respiration (Fig 2f) trended toward an increase in the moderate RV hypertrophy group (with preserved RV systolic function), and decreased in the severe RV hypertrophy and RV failure groups (oxidative phosphorylation: moderate RV hypertrophy 287.6±19.75 vs. RV failure 137.8±11.57 pmol/(sec*ml), p=0.0003) (uncoupled respiration: moderate RV hypertrophy 446.8±26.13 vs. RV failure 254.5±25.1 pmol/(sec*ml), p=0.0006). The respiratory control ratio (Fig 2g) trended toward an increase in moderate hypertrophy and decreased in severe hypertrophy and RV failure (RCR: moderate RV hypertrophy 4.05±0.49 vs. RV failure 2.47±0.16 pmol/(sec*ml), p=0.0079). The cohort of patients with end stage RV failure was too small to correlate increasing 4HNE expression with the acuity of illness, duration of heart failure, medication use, or mitochondrial respiration. We tested whether the increased oxygen consumption seen in moderate RV hypertrophy could have been influenced by the higher percent of infants in this group. Children with moderate RV hypertrophy <1 year vs. >1 year of age (mean age 0.32±0.1 vs. 5.37±5.1 years) showed no difference in oxidative phosphorylation (312.9±34.41 vs. 262.2±15.8, p=0.161) (Fig 2h). Similarly, linear regression analysis of oxidative phosphorylation and age (Fig 2i) demonstrated a low R^2 at 0.32 suggesting that although age does play a role, it is responsible for only about 1/3rd of the variation in oxidative phosphorylation. The slope of the line representing the actual change per year in oxidative phosphorylation was very low at −4.23 pmol/(sec*ml) ($y = -4.23 + 260.7$; $R^2 = 0.32$, p=0.007), suggesting that while age does play a small role in changes in oxidative phosphorylation, the changes we describe with RV failure are greater. Similarly aged patients also had higher oxidative phosphorylation in moderate RV hypertrophy compared to RV failure. We also performed multiple regression analysis to understand the relationship between oxidative phosphorylation, patient's age, and disease categories (mild/moderate/

severe RV hypertrophy and RV failure). Age was not independently associated with oxidative phosphorylation (−2.1, 95% CI [−5.14, 0.91], p=0.158), while moderate hypertrophy was independently associated with oxidative phosphorylation (132.8, 95% CI [69.14, 196.4], p=0.0004). The model was able to account for 70% of the variance in oxidative phosphorylation (R^2 = 0.6986, p = 0.0004).

Mitochondrial mass is not decreased in RV hypertrophy and RV failure

We investigated whether mitochondrial mass decreased in RV failure thereby leading to a decrease in oxidative phosphorylation. Mitochondrial mass (measured by VDAC1 expression) and biogenesis (measured by PGC1α expression) were not decreased but actually trended toward being increased in RV failure (Fig 3a–c). As further evidence of maintained to increased mitochondrial biogenesis, mitochondrial DNA (mtDNA) was also assessed. mtDNA was not depleted as previously described for RV hypertrophy and RV failure[19], but instead was increased with RV failure (moderate RV hypertrophy 356.5±28.85 vs. RV failure 960±180.6, p=0.025) (Fig 3d). mtDNA copy number was very variable in patients with RV failure.

RV failure is characterized by abnormal mitochondrial morphology and disruption in network connectivity

We next assessed mitochondrial structure in RV failure using TEM. Severe RV hypertrophy samples were not available for TEM. Mitochondria were divided into 0.1 μm^2 size bins and a histogram was developed to evaluate mitochondrial size distribution (Fig 3e). Substantial heterogeneity was noted in mitochondrial size in all groups, however the size distribution and median mitochondrial size (Fig 3f) was not different between groups. Qualitatively, mitochondria lost their elongated shape and became more circular in moderate RV hypertrophy and more irregularly shaped in RV failure with decrease in cristae density and loss of network connectivity (Fig 3g). Substantial heterogeneity was also noted in mitochondrial dynamics proteins, however the expression of fission protein DRP1 trended toward an increase and fusion protein MFN2 increased in RV failure (Supplemental Results) (Supplemental Fig II).

4HNE treatment attenuates oxidative phosphorylation-mediated ATP synthesis

Having shown an association between increased 4HNE-adduction of mitochondrial enzymes, impaired oxidative phosphorylation, and mitochondrial structural changes, we next evaluated whether treatment with 4HNE can directly impair oxidative phosphorylation using HL1 cardiomyocytes and confirmed important changes in hiPSC-CM. We first tested whether the systemic inotropic medications used in the RV failure patients such as the β adrenoreceptor agonist epinephrine could have caused the increase in 4HNE-adduction. Commonly used in vitro β adrenoreceptor agonists norepinephrine and isoproterenol were used to treat HL1 cells and did not increase 4HNE expression (Supplemental Fig IIIa, b).

4HNE treatment resulted in increased formation of multiple 4HNE protein adducts similar to those seen in patients (Fig 4a, b) and decreased cell count (Fig 4c). In order to better evaluate which proteins underwent 4HNE-adduction, proteins with increased 4HNE-adduction were detected in 4HNE treated HL1 cardiomyocytes by 2D-gel electrophoresis

and western blot and then identified using mass spectrometry and compared with control (Supplemental Fig IVa, b). Fifteen 4HNE adducted proteins which increased in 4HNE treated cells (≥1.6 fold change) were selected for identification (Supplemental Table III). Interestingly, six of the fifteen proteins were metabolic pathway proteins and most were directly related to mitochondrial metabolism similar to that seen in patient RV failure including proteins involved in electron transport chain activity and mitochondrial respiration such as NADH dehydrogenase, cytochrome b, and cytochrome c. In addition, mitochondrial proteins involved in survival and stress-response were targeted by 4HNE similar to that seen in patient RV failure. 4HNE adduction to proteins involved in mitochondrial respiration was associated with decreased oxygen consumption (Fig 4d–h). Of note, 4HNE decreased respiratory control ratio (control 3.383±0.0565 vs. 50 μM 4HNE 2.783±0.0766, $p<0.0057$) despite increased mitochondrial membrane potential, indicating 4HNE attenuates oxidative phosphorylation by inhibiting the electron transport chain activity rather than by an increase in mitochondrial membrane leakage (Fig 4i–k). The effect of 4HNE on mitochondrial respiration was confirmed in hiPSC-CM (Supplemental Fig Va–d). Similar to HL-1 cells, 4HNE decreased oxygen consumption and respiratory control ratio in hiPSC-CMs (Supplemental Fig Ve, f).

Carvedilol does not rescue 4HNE mediated attenuation of ATP synthesis

We next evaluated whether treatment with carvedilol can rescue 4HNE mediated impairment of oxidative phosphorylation in HL1 cardiomyocytes since Carvedilol is a knownn antioxidant, decreasing lipid peroxidation and 4HNE in ischemic and dilated cardiomyopathy[13, 14]. Carvedilol decreased 4HNE protein adducts but did not improve oxygen consumption to baseline levels. However, mass spectrometry identified proteins involved in electron transport chain activity and mitochondrial respiration such as NADH dehydrogenase, cytochrome b, and cytochrome c to be highly adducted to 4HNE despite carvedilol treatment, similar to that seen with 4HNE alone (Supplemental Table III). This may explain the lack of improvement in oxygen consumption. Although carvedilol also increased the mitochondrial membrane potential, this is likely to be spurious based on the observation that leak respiration did not decrease concomitantly with the carvedilol-mediated increase in mitochondrial membrane potential. This may be detecting the deprotonated, negatively charged form of carvedilol in the high pH matrix environment[20, 21], rather than change in the hydrogen ion concentration gradient (Supplemental Fig VI).

4HNE increased mitochondrial mass and alters mitochondrial structure

4HNE increased mitochondrial mass in HL1 cells by MitoTracker Red CMXRos fluorescence: control 4212±306.9 vs. 4HNE 9817±212.4, $p<0.0001$ (Fig 5a, b) and VDAC1 expression: control 1±0.03 vs. 4HNE 2.13±0.04, $p<0.0001$ (Fig 5c, d), even though it did not affect mitochondrial biogenesis as indicated by unchanged PGC1α expression (Fig 5e). Fluorescence microscopy demonstrated no change in mitochondrial area with 4HNE (Figure 6a–c). However, 4HNE decreased mitochondrial perimeter (Fig 6d) and increased mitochondrial circularity making them more compact and increased solidity leading to less surface ruffling (Fig 6e, f). Carvedilol did not change mitochondrial morphology. 4HNE treatment increased the whole-cell expression of fission proteins (Supplement Fig VIIa–g). In contrast, despite whole-cell level increase in fission proteins, mitochondrial localization

of the fission and fusion proteins were inhibited by 4HNE (Supplemental Fig VIIh–n) (Supplemental Results).

Discussion

For many children with congenital heart disease or pulmonary hypertension, pressure overload stress on the RV exists throughout life, even after successful surgical repair or palliation leading to RV hypertrophy and dilation and eventually RV failure[3, 22]. We focused on the dysregulation of myocardial energy generation as a driver for the development of RV failure in children with congenital heart disease with RV pressure overload. We show that RV failure is characterized by increased 4HNE-adduction of metabolic and mitochondrial proteins. This was associated with decreased myocardial energy generation and mitochondrial structural disruption with increasing severity of RV hypertrophy and RV failure. Mechanistically, we show that 4HNE is sufficient to decrease energy generation by inhibiting electron transport chain complex activities and mitochondrial dynamics.

Increased oxidative stress has been shown in RV pressure overload due to pulmonary hypertension[23, 24], and in left ventricular hypertrophy[25], but no data exists on the post translational modification of mitochondrial enzymes by 4HNE and its effects in RV hypertrophy and failure. We show that whereas all patients with RV failure demonstrate increased lipid peroxidation, there is significant inter-patient variability. We speculate that the duration and severity of heart failure as well as the use of systemic inotropic agents can influence the degree of oxidative stress[26, 27]. 4HNE-induced oxidative stress has previously been recognized in the left ventricle with ischemic heart disease due to myocardial infarction[28], doxorubicin cardiotoxicity[29] and dilated cardiomyopathy[14]. Cardiomyocyte mitochondria can be damaged not only by the 4HNE generated locally but also by exogenous 4HNE[30], such as circulating 4HNE seen in heart failure patients[31]. Zhao et al. identified several 4HNE-adducted mitochondrial proteins in a preclinical murine model of doxorubicin cardiotoxicity and demonstrated decreased activity of the electron transport chain[10, 11, 32]. We show for the first time an increase in 4HNE adduction preferentially targeting metabolic and mitochondrial proteins in the myocardium in pressure overload-induced RV failure in children with congenital heart disease. 4HNE-mediated damage in the failing RV not only decreases electron transport chain activity, thereby generating less energy, but also adducts to sarcomeric proteins, cytoskeletal proteins and pro-survival proteins, all of which may work in concert leading to a heart failure phenotype. This data provides valuable insight into the pathological changes in the RV that may trigger and/or exacerbate RV failure.

We show that although moderate RV hypertrophy demonstrates a trend toward a potential compensatory upregulation of mitochondrial energy generation, this is lost with increasing severity of RV hypertrophy, which may be a precursor to the development of RV failure. The decrease in oxidative phosphorylation occurs despite preserved mitochondrial mass and despite increased cardiac workload with hypertrophy and heart failure. The decrease in oxidative phosphorylation could serve as a marker for the need for earlier intervention to relieve RV pressure overload and preserve long-term RV function. The decrease in oxygen consumption seen in severe hypertrophy could also be related to the longer duration of

hypertrophy, suggesting that sustained cardiac hypertrophy may cause a dysfunctional mitochondrial phenotype similar to that seen in cardiac aging. This is comparable to work by Karamanlidis et al.[19] showing preserved mitochondrial activity in RV hypertrophy with preserved RV function and impaired mitochondrial activity in children with RV failure. However, while Karamanlidis et al. indirectly measured mitochondrial activity by citrate synthase and succinate dehydrogenase activities, we show a direct high-resolution measurement of mitochondrial respiration as a function of both electron transport chain complex activities (rates of proton gradient generation and electron transfer) and mitochondrial membrane integrity (proton leak).

Lipid peroxidation is also known to damage mitochondrial DNA[33, 34], which is essential for mitochondrial biogenesis[35, 36]. The increase in mitochondrial DNA copy number seen in RV failure may be related to the oxidative stress-induced upregulation of mitochondrial DNA synthesis[37]. This differs from that reported by Karamanlidis et al[19] who demonstrated a progressive decrease in mitochondrial biogenesis in children with RV pressure overload from hypertrophy to failure. The differences seen in our study may be related to the different group of patients with RV failure, namely single ventricle in their study and a biventricular circulation in ours and to the high levels of lipid peroxidation seen in our patients. Furthermore, the difference in patient ages may be a confounding factor. Whereas the RV failure patients studied by Karamanlidis et al. were very young (range: 0.1 to 1.5 years), the average age of our RV failure patients was 10.9±6.9 years.

Mechanistically, we show the direct effects of 4HNE on cardiomyocyte energy generation to implicate its role in the development of RV failure, where 4HNE decreases oxygen consumption by inhibiting the electron transport chain complexes and inhibiting fission and fusion. In pathologic patient brain and plasma, 4HNE concentrations can increase to between 1 and 10 μM, and in some cases, even up to 100 μM[38, 39]. As such, *in vivo* cardiomyocyte mitochondria can be damaged not only by the 4HNE generated locally but also by exogenous 4HNE[30], such as circulating 4HNE seen in heart failure patients[31]. Of note, although the concentration of 4HNE we have used in our study (50 μM) is still physiologically relevant, it exceeds the typically observed *in vivo* 4HNE levels. However, with this high concentration, we were able to show that 4HNE has acute dysregulatory effects on the mitochondrial function. Interestingly, among these effects, 4HNE also increased mitochondrial mass. This is consistent with previously reported findings that knockout of both fission and fusion proteins in the heart leads to increased mitochondrial mass[40]. 4HNE-induced mitochondrial membrane hyperpolarization[41–43] can further exacerbate lipid peroxidation, mitochondrial damage, and cell death, all of which have previously been shown in end stage ischemic heart failure in adults[44]. Our *in vitro* model does not fully recapitulate the human heart failure phenotype due to the lack of various *in vivo* stressors such as pressure overload and hypoxia. However, it provides insight into the effect of exogenous 4HNE on cardiomyocyte function.

Our data provide a rationale for developing drugs to mitigate lipid peroxidative damages. Carvedilol is one of the mainstays in clinical heart failure therapy and has shown promise in pulmonary hypertension induced RV failure[45]. While the ability of carvedilol to reduce lipid peroxidation has been reported[14, 46–48], it is not known whether it can also confer protection

against reactive lipid peroxidation products. Carvedilol inhibited overall 4HNE-adduction, but many mitochondrial and metabolic proteins remained adducted to 4HNE; thus, while carvedilol has antioxidant properties, it was unable to rescue 4HNE-mediated decrease in mitochondrial energy generation. However, under basal conditions, carvedilol leads to a favorable mitochondrial phenotype by decreasing fission, increasing fusion, increasing mitochondrial mass and improving mitochondrial membrane potential, suggesting that this may still be beneficial in patients at risk for the development of heart failure.

Conclusion

Metabolic, mitochondrial, and key sarcomeric and cytoskeletal proteins are susceptible to 4HNE-adduction in RV failure. This is associated with impaired mitochondrial energy generation even in severe RV hypertrophy prior to the development of RV dysfunction and RV failure in patients with RV pressure overload. Mechanistically, we show that 4HNE impairs myocardial energy generation by inhibiting electron transport chain complexes and inhibiting mitochondrial dynamics. Carvedilol could not rescue the 4HNE-mediated impairment in energy generation. Strategies to decrease lipid peroxidation may improve myocardial energy generation and thereby preserve long-term heart function in patients with congenital heart disease. As surgical techniques for repair of complex congenital heart lesions continue to improve, long-term survival and quality of life will increasingly depend on our ability to preserve long-term RV function.

Supplementary Material

Refer to Web version on PubMed Central for supplementary material.

Acknowledgments

The JEOL JEM1400 electron microscope at the Cell Sciences Imaging Facility of Stanford University was funded by a NIH Shared Instrumentation grant (William Talbot, PI; installation date, 01/2011) and the American Recovery and Reinvestment Act award 1S10RR026780–01 from the National Center for Research Resources (NCRR). The manuscripts contents are solely the responsibility of the authors and do not necessarily represent the official views of the NCRR or the NIH.

We thank our human subjects research coordinators Sara Sherman-Levine and Aihua Zhu, supported by NIH/National Center for Advancing Translational Sciences/Clinical and Translational Science Awards grant UL1 TR001085, the Lucile Packard Foundation for Children’s Health, and the Child Health Research Institute. We thank Helen Lu for the analysis of the EM data. The authors thank Julia Ryan for technical assistance with iPSC maintenance and cardiac differentiation.

We thank the pediatric congenital cardiac surgeons, Drs Frank Hanley, Mohan Reddy, Katsuhide Meada and Michael Ma, the surgical physician assistant team and the operating room nursing staff for the patient myocardial samples.

Funding

K08 HL127277–01 NIH to SR; Reddy Foundation grant to SR; Department of Defense PR151448 to DB and SR; NIH K08HL148553 to SLP.

Non-standard Abbreviations and Acronyms

RV	Right ventricle

4HNE	4-hydroxynonenal
ATP	Adenosine triphosphate
RV FAC	Fractional area change
VDAC1	Voltage-dependent anion-selective channel protein 1
PGC1α	PPARG coactivator 1$^{\alpha}$
DRP1	Dynamin 1-like
MFF	Mitochondrial fission factor
OPA1	Mitochondrial dynamin like GTPase
MFN2	Mitofusin 2
TOM20	Translocase of outer mitochondrial membrane 20
RCR	Respiratory control ratio
FCCP	Carbonyl cyanide-p-trifluoromethoxyphenylhydrazone
hiPSC-CM	Human induced pluripotent stem cell-derived cardiomyocytes
TEM	Transmission electron microscopy
mtDNA	Mitochondrial DNA

References

1. Altmann K, Printz BF, Solowiejczyk DE, Gersony WM, Quaegebeur J and Apfel HD. Two-dimensional echocardiographic assessment of right ventricular function as a predictor of outcome in hypoplastic left heart syndrome. Am J Cardiol. 86:964–968. [PubMed: 11053708]
2. Bogaard HJ, Abe K, Vonk Noordegraaf A and Voelkel NF. The right ventricle under pressure: cellular and molecular mechanisms of right-heart failure in pulmonary hypertension. Chest. 2009;135:794–804. [PubMed: 19265089]
3. Fine NM, Chen L, Bastiansen PM, Frantz RP, Pellikka PA, Oh JK and Kane GC. Outcome prediction by quantitative right ventricular function assessment in 575 subjects evaluated for pulmonary hypertension. Circ Cardiovasc Imaging. 2013;6:711–721. [PubMed: 23811750]
4. Haddad F, Hunt SA, Rosenthal DN and Murphy DJ. Right ventricular function in cardiovascular disease, part I: Anatomy, Physiology, Aging, and Functional Assessment of the Right Ventricle. Circulation. 2008;117:1436–1448. [PubMed: 18347220]
5. Reddy S, Bernstein D and Newburger JW. Renin-Angiotensin-Aldosterone System Inhibitors for Right Ventricular Dysfunction in Tetralogy of Fallot: Quo Vadis? Circulation. 2018;137:1472–1474. [PubMed: 29610128]
6. Weiss RG, Gerstenblith G and Bottomley PA. ATP flux through creatine kinase in the normal, stressed, and failing human heart. Proc Natl Acad Sci U S A. 2005;102:808–813. [PubMed: 15647364]
7. Ide T, Tsutsui H, Kinugawa S, Utsumi H, Kang D, Hattori N, Uchida K, Arimura KI, Egashira K and Takeshita A. Mitochondrial eectron transport complex I is a potential source of oxygen free radicals in the failing myocardium. Circ Res. 1999;85:357–363. [PubMed: 10455064]

8. Srivastava S, Chandrasekar B, Bhatnagar A and Prabhu SD. Lipid peroxidation-derived aldehydes and oxidative stress in the failing heart: role of aldose reductase. Am J Physiol Heart Circ Physiol. 2002;283:H2612–H2619. [PubMed: 12388223]
9. Lucas DT and Szweda LI. Cardiac reperfusion injury: Aging, lipid peroxidation, and mitochondrial dysfunction. Proc Natl Acad Sci U S A. 1998;95:510–514. [PubMed: 9435222]
10. Chen J, Schenker S, Frosto TA and Henderson GI. Inhibition of cytochrome c oxidase activity by 4-hydroxynonenal (HNE): Role of HNE adduct formation with the enzyme subunits. Biochim Biophys Acta Gen Subj. 1998;1380:336–344.
11. Petersen DR and Doorn JA. Reactions of 4-hydroxynonenal with proteins and cellular targets. Free Radic Biol Med. 2004;37:937–945. [PubMed: 15336309]
12. Anderson EJ, Katunga LA and Willis MS. Mitochondria as a source and target of lipid peroxidation products in healthy and diseased heart. Clin Exp Pharmacol Physiol. 2012;39:179–193. [PubMed: 22066679]
13. Moreno AJ, Santos DJ and Palmeira CM. Ischemic heart disease: the role of mitochondria--carvedilol prevents lipid peroxidation of mitochondrial membranes. Rev Port Cardiol. 1998;17 Suppl 2:Ii63–77. [PubMed: 9835783]
14. Nakamura K, Kusano K, Nakamura Y, Kakishita M, Ohta K, Nagase S, Yamamoto M, Miyaji K, Saito H, Morita H, et al. Carvedilol decreases elevated oxidative stress in human failing myocardium. Circulation. 2002;105:2867–2871. [PubMed: 12070115]
15. Cordero-Reyes AM, Gupte AA, Youker KA, Loebe M, Hsueh WA, Torre-Amione G, Taegtmeyer H and Hamilton DJ. Freshly isolated mitochondria from failing human hearts exhibit preserved respiratory function. J Mol Cell Cardiol. 2014;68:98–105. [PubMed: 24412531]
16. Nowak G, Bakajsova D and Clifton GL. Protein kinase C-ϵ modulates mitochondrial function and active Na+ transport after oxidant injury in renal cells. Am J Physiol Renal Physiol. 2004;286:F307–F316. [PubMed: 14570699]
17. Jastroch M, Divakaruni AS, Mookerjee S, Treberg JR and Brand MD. Mitochondrial proton and electron leaks. Essays Biochem. 2010;47:53–67. [PubMed: 20533900]
18. Schindelin J, Arganda-Carreras I, Frise E, Kaynig V, Longair M, Pietzsch T, Preibisch S, Rueden C, Saalfeld S and Schmid B. Fiji: an open-source platform for biological-image analysis. Nat Methods. 2012;9:676. [PubMed: 22743772]
19. Karamanlidis G, Bautista-Hernandez V, Fynn-Thompson F, del Nido P and Tian R. Impaired mitochondrial biogenesis precedes heart failure in right ventricular hypertrophy in congenital heart disease. Circ Heart Fail. 2011;4:707–713. [PubMed: 21840936]
20. Oliveira PJ, Marques MPM, Batista de Carvalho LAE and Moreno AJM. Effects of carvedilol on isolated heart mitochondria: evidence for a protonophoretic mechanism. Biochem Biophys Res Commun. 2000;276:82–87. [PubMed: 11006086]
21. Soleymanpour A and Ghasemian M. Chemically modified carbon paste sensor for the potentiometric determination of carvedilol in pharmaceutical and biological media. Measurement. 2015;59:14–20.
22. Therrien J, Siu SC, McLaughlin PR, Liu PP, Williams WG and Webb GD. Pulmonary valve replacement in adults late after repair of tetralogy of fallot: are we operating too late? J Am Coll Cardiol. 2000;36:1670–1675. [PubMed: 11079675]
23. Pichardo J, Palace V, Farahmand F and Singal PK. Myocardial oxidative stress changes during compensated right heart failure in rats. Mol Cell Biochem. 1999;196:51–57. [PubMed: 10448902]
24. Redout EM, Toorn Avd, Zuidwijk MJ, Kolk CWAvd, Echteld CJAv, Musters RJP, Hardeveld Cv, Paulus WJ and Simonides WS. Antioxidant treatment attenuates pulmonary arterial hypertension-induced heart failure. Am J Physiol Heart Circ Physiol. 2010;298:H1038–H1047. [PubMed: 20061549]
25. Dolinsky VW, Chan AYM, Frayne IR, Light PE, Rosiers CD and Dyck JRB. Resveratrol Prevents the Prohypertrophic Effects of Oxidative Stress on LKB1. Circulation. 2009;119:1643–1652. [PubMed: 19289642]
26. Rathore N, John S, Kale M and Bhatnagar D. Lipid peroxidation and antioxidant enzymes in isoproterenol induced oxidative stress in rat tissues. Pharmacol Res. 1998;38:297–303. [PubMed: 9774493]

27. Mari Kannan M and Darlin Quine S. Ellagic acid protects mitochondria from β-adrenergic agonist induced myocardial damage in rats; evidence from in vivo, in vitro and ultra structural study. Food Res Int. 2012;45:1–8.
28. Campos JC, Queliconi BB, Dourado PM, Cunha TF, Zambelli VO, Bechara LR, Kowaltowski AJ, Brum PC, Mochly-Rosen D and Ferreira JC. Exercise training restores cardiac protein quality control in heart failure. PLoS One. 2012;7:e52764.
29. Zhao Y, Miriyala S, Miao L, Mitov M, Schnell D, Dhar SK, Cai J, Klein JB, Sultana R, Butterfield DA, et al. Redox proteomic identification of HNE-bound mitochondrial proteins in cardiac tissues reveals a systemic effect on energy metabolism after doxorubicin treatment. Free Radic Biol Med. 2014;72:55–65. [PubMed: 24632380]
30. Hill BG, Dranka BP, Zou L, Chatham JC and Darley-Usmar VM. Importance of the bioenergetic reserve capacity in response to cardiomyocyte stress induced by 4-hydroxynonenal. Biochem J. 2009;424:99–107. [PubMed: 19740075]
31. Mak S, Lehotay DC, Yazdanpanah M, Azevedo ER, Liu PP and Newton GE. Unsaturated aldehydes including 4-OH-nonenal are elevated in patients with congestive heart failure. J Card Fail. 2000;6:108–114. [PubMed: 10908084]
32. Xiao M, Zhong H, Xia L, Tao Y and Yin H. Pathophysiology of mitochondrial lipid oxidation: Role of 4-hydroxynonenal (4-HNE) and other bioactive lipids in mitochondria. Free Radic Biol Med. 2017;111:316–327. [PubMed: 28456642]
33. Almeida AM, Bertoncini CR, Borecky J, Souza-Pinto NC and Vercesi AE. Mitochondrial DNA damage associated with lipid peroxidation of the mitochondrial membrane induced by Fe2+-citrate. An Acad Bras Cienc. 2006;78:505–514. [PubMed: 16936939]
34. Hruszkewycz AM. Evidence for mitochondrial DNA damage by lipid peroxidation. Biochem Biophys Res Commun. 1988;153:191–197. [PubMed: 2837198]
35. Chen L, Gong Q, Stice JP and Knowlton AA. Mitochondrial OPA1, apoptosis, and heart failure. Cardiovasc Res. 2009;84:91–99. [PubMed: 19493956]
36. Tian L, Neuber-Hess M, Mewburn J, Dasgupta A, Dunham-Snary K, Wu D, Chen KH, Hong Z, Sharp WW, Kutty S, et al. Ischemia-induced Drp1 and Fis1-mediated mitochondrial fission and right ventricular dysfunction in pulmonary hypertension. J Mol Med (Berl). 2017;95:381–393. [PubMed: 28265681]
37. Lee HC and Wei YH. Mitochondrial biogenesis and mitochondrial DNA maintenance of mammalian cells under oxidative stress. Int J Biochem Cell Biol. 2005;37:822–834. [PubMed: 15694841]
38. Dodson M, Wani WY, Redmann M, Benavides GA, Johnson MS, Ouyang X, Cofield SS, Mitra K, Darley-Usmar V and Zhang J. Regulation of autophagy, mitochondrial dynamics, and cellular bioenergetics by 4-hydroxynonenal in primary neurons. Autophagy. 2017;13:1828–1840. [PubMed: 28837411]
39. Strohmaier H, Hinghofer-Szalkay H and Jörg Schaur R. Detection of 4-hydroxynonenal (HNE) as a physiological component in human plasma. J Lipid Mediat Cell Signal. 1995;11:51–61. [PubMed: 7728417]
40. Song M, Franco A, Fleischer JA, Zhang L and Dorn GW 2nd. Abrogating Mitochondrial Dynamics in Mouse Hearts Accelerates Mitochondrial Senescence. Cell Metab. 2017;26:872–883.e5. [PubMed: 29107503]
41. Jheng HF, Tsai PJ, Guo SM, Kuo LH, Chang CS, Su IJ, Chang CR and Tsai YS. Mitochondrial fission contributes to mitochondrial dysfunction and insulin resistance in skeletal muscle. Mol Cell Biol. 2012;32:309–319. [PubMed: 22083962]
42. Disatnik MH, Ferreira Julio CB, Campos Juliane C, Gomes Kátia S, Dourado Paulo MM, Qi X and Mochly-Rosen D. Acute inhibition of excessive mitochondrial fission after myocardial infarction prevents long-term cardiac dysfunction. J Am Heart Assoc. 2:e000461.
43. Lee YJ, Jeong SY, Karbowski M, Smith CL and Youle RJ. Roles of the mammalian mitochondrial fission and fusion mediators Fis1, Drp1, and Opa1 in apoptosis. Mol Biol Cell. 2004;15:5001–5011. [PubMed: 15356267]
44. Sabbah HN. Apoptotic cell death in heart failure. Cardiovasc Res. 2000;45:704–712. [PubMed: 10728392]

45. Grinnan D, Bogaard HJ, Grizzard J, Tassell BV, Abbate A, DeWilde C, Priday A and Voelkel NF. Treatment of Group I Pulmonary Arterial Hypertension with Carvedilol Is Safe. Am J Respir Crit Care Med. 2014;189:1562–1564. [PubMed: 24930531]

46. Huang H, Shan J, Pan XH, Wang HP, Qian LB and Xia Q. Carvedilol improved diabetic rat cardiac function depending on antioxidant ability. Diabetes Res Clin Pract. 2007;75:7–13. [PubMed: 16780994]

47. Kumar A, Dogra S and Prakash A. Effect of carvedilol on behavioral, mitochondrial dysfunction, and oxidative damage against d-galactose induced senescence in mice. Naunyn Schmiedebergs Arch Pharmacol. 2009;380:431–441. [PubMed: 19685040]

48. Sahu BD, Koneru M, Bijargi SR, Kota A and Sistla R. Chromium-induced nephrotoxicity and ameliorative effect of carvedilol in rats: Involvement of oxidative stress, apoptosis and inflammation. Chem Biol Interact. 2014;223:69–79. [PubMed: 25245570]

49. Burridge PW, Matsa E, Shukla P, Lin ZC, Churko JM, Ebert AD, Lan F, Diecke S, Huber B, Mordwinkin NM, et al. Chemically defined generation of human cardiomyocytes. Nat Methods. 2014;11:855–860. [PubMed: 24930130]

50. Sharma A, Li G, Rajarajan K, Hamaguchi R, Burridge PW and Wu SM. Derivation of highly purified cardiomyocytes from human induced pluripotent stem cells using small molecule-modulated differentiation and subsequent glucose starvation. J Vis Exp. 2015:52628.

Clinical Perspective

What is new?

- We show that right ventricular failure is characterized by increased oxidation of membrane phospholipids, known as lipid peroxidation and its products such as 4-hydroxynonenal (4HNE).
- 4HNE binds to metabolic and mitochondrial proteins and was associated with decreased myocardial energy generation and mitochondrial structural disruption with increasing severity of right ventricular hypertrophy and right ventricular failure.
- Mechanistically, we show that 4HNE is sufficient to decrease energy generation by inhibiting electron transport chain complex activities and mitochondrial dynamics.

What are the Clinical Implications?

- The mechanisms of congenital heart disease-associated right ventricular dysfunction are not well known, limiting the availability of therapeutic approaches.
- Since standard heart failure therapies such as angiotensin-converting enzyme inhibitors and beta blockers are ineffective in the treatment of RV failure, developing therapies focusing on new targets such as lipid peroxidation could improve right ventricular function in congenital heart diseases by improving mitochondrial energy generation and cardiomyocyte survival.

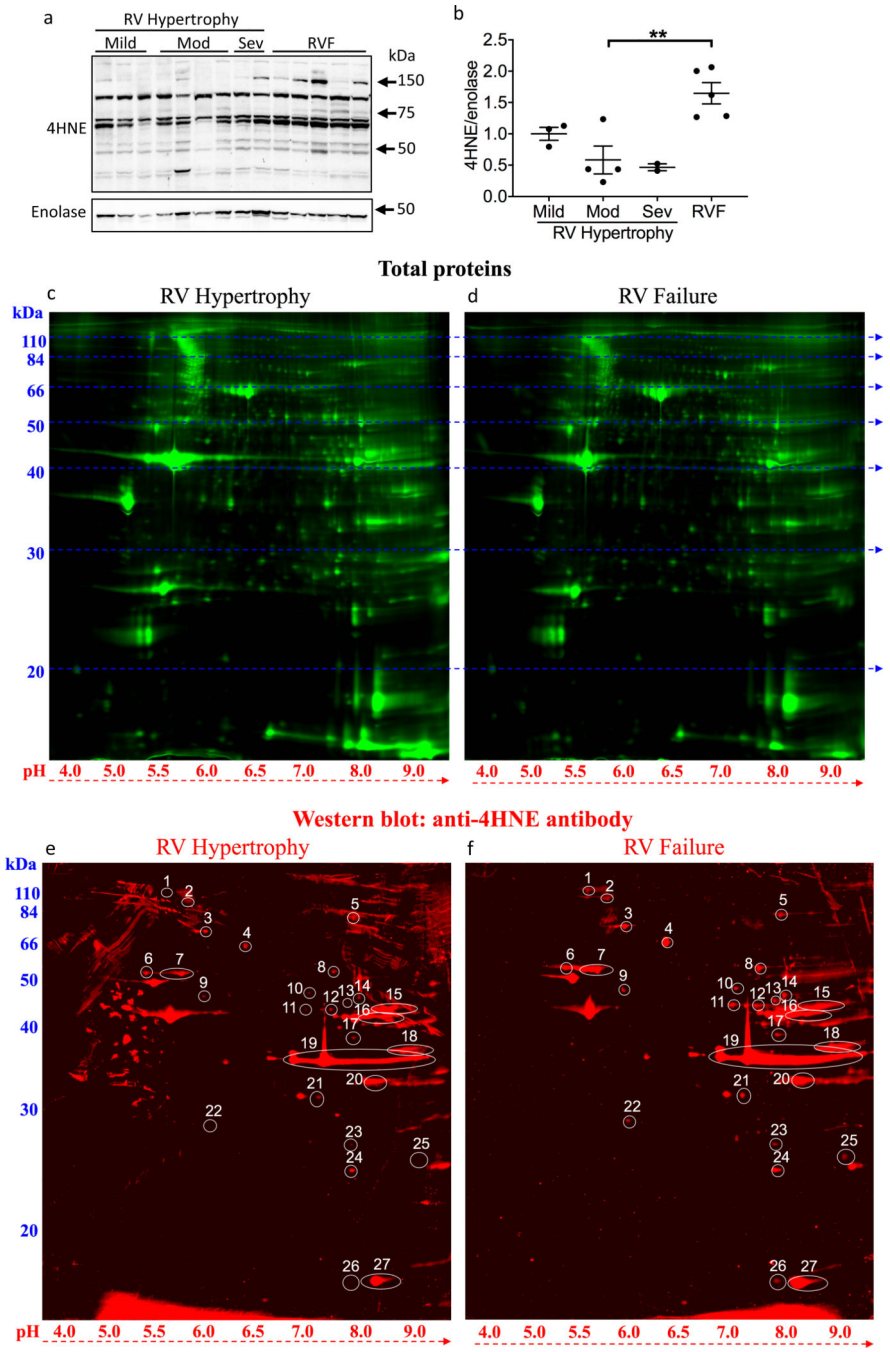

Figure 1.

Lipid peroxidation is increased in RV failure. (a, b) 4HNE adducts increased with RV failure vs moderate RV hypertrophy, N=2–5/group. (c, d) 2D-gel electrophoresis and western blot were used to detect total protein in representative RV hypertrophy (N=1) and RV failure (N=1) samples. (e, f) 2D-gel electrophoresis and western blot were used to detect the proteins with increased 4HNE-adducts. 27 protein spots where 4HNE signals were higher in RV failure vs. RV hypertrophy were numbered for identification. Mod – moderate; Sev –

severe; RV – right ventricle; RVF – right ventricular failure; 4HNE - 4-hydroxynonenal. Data are presented as mean±SEM. **p<0.01.

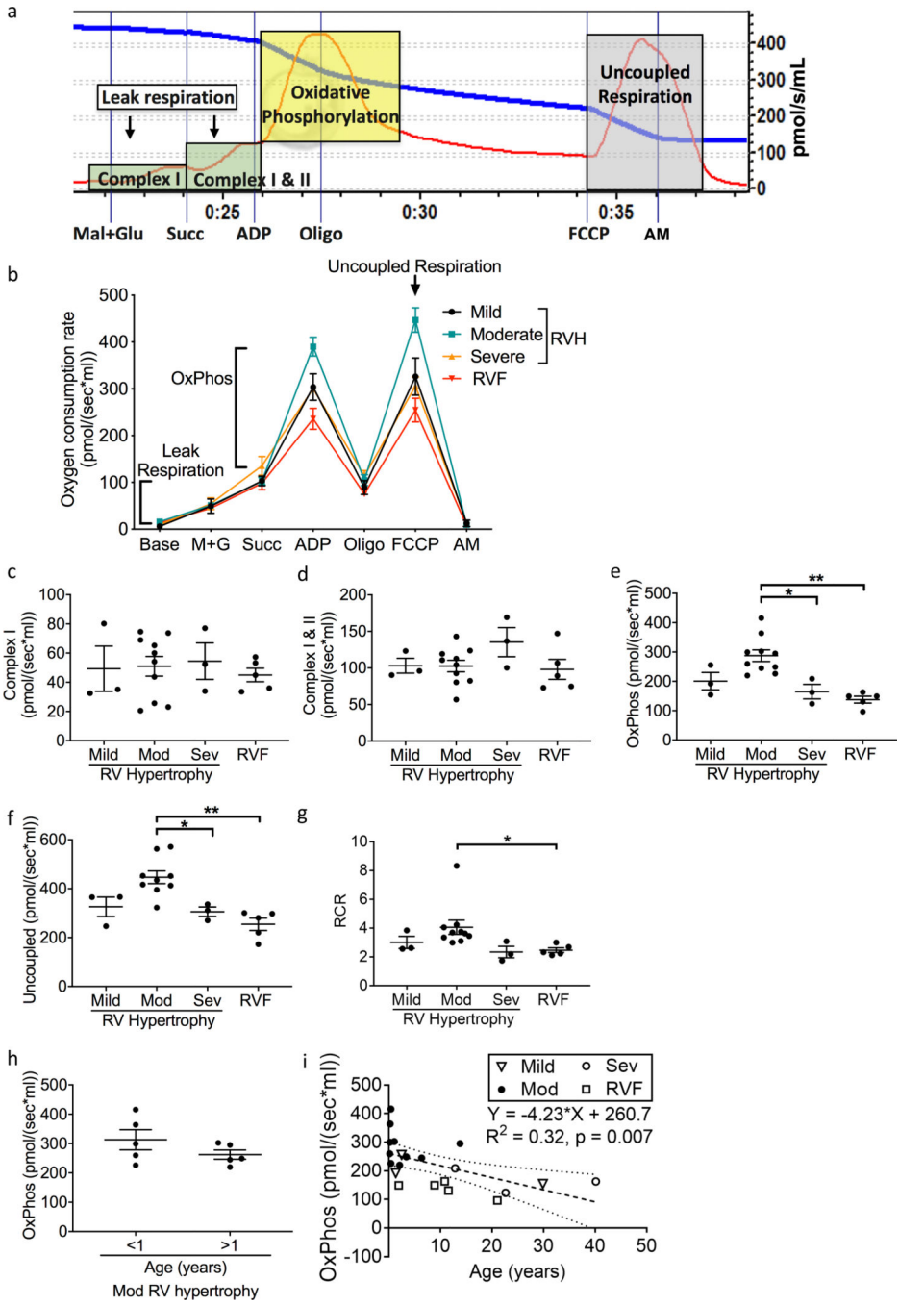

Figure 2.

Patients with severe RV hypertrophy and RV failure demonstrate decreased oxidative phosphorylation. (a) A representative oxygen consumption tracing is shown for myocardial tissue (red curve) along with the available oxygen in the assay chamber (blue curve). We evaluated leak respiration (green shaded zones), oxidative phosphorylation (yellow shaded zone), and uncoupled respiration (gray shaded zone). (b) Summary of oxygen consumption in right ventricular myocardial tissue (N=3–10/group). (c, d) Complex I and Complex II mediated oxygen consumption was unchanged across all groups. (e, f) Oxidative

phosphorylation and uncoupled respiration trended toward an increase from mild to moderate RV hypertrophy, decreased from moderate RV hypertrophy to severe hypertrophy, and decreased with RV failure. Oxidative phosphorylation remained significantly decreased after adjusting for age (p=0.0004) in RV failure. (g) Similarly, respiratory control ratio trended toward an increase in moderate hypertrophy and subsequently significantly decreased from moderate RV hypertrophy to RV failure. (h) Oxidative phosphorylation did not differ in patients with moderate RV hypertrophy between those <1 year of age versus >1 year of age (N=5/group). (i) Linear regression analysis demonstrates that age plays a role in the changes seen in oxidative phosphorylation but the actual change in oxidative phosphorylation per year (Slope) is small at −4.23pmol/sec*ml (N=21). RV – right ventricle; RVF – right ventricular failure; M+G – malate and glutamate; Succ – succinate; Oligo – oligomycin; FCCP - carbonyl cyanide-p-trifluoromethoxyphenylhydrazone; AM – antimycin A; Mod – moderate; Sev – severe; OxPhos - oxidative phosphorylation; RCR – respiratory control ratio. Data are presented as mean±SEM. *p<0.05, **p<0.01.

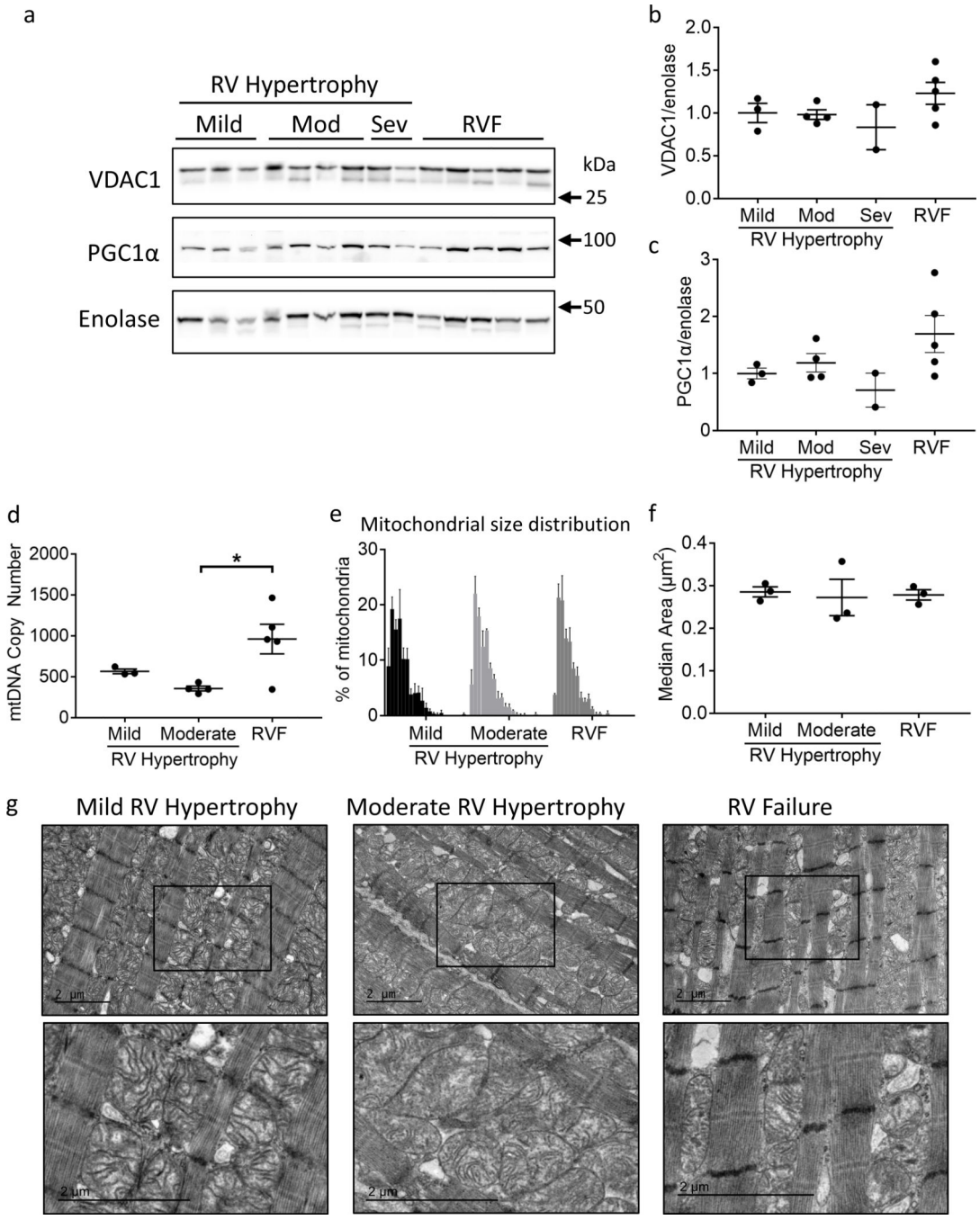

Figure 3.

Patients with RV failure demonstrate mitochondrial structural changes. (a-c) Both VDAC1 (mitochondrial protein) and PGC1α (mitochondrial biogenesis factor) trended toward an increase in RV failure (N=2–5/group). (d) Mitochondrial DNA copy number was not different between mild and moderate RV hypertrophy groups, but was significantly increased from moderate RV hypertrophy to RV failure (N=3–5/group). (e) Histogram of mitochondrial size distribution for each group by transmission electron microscopy demonstrates no difference in mitochondrial size. Each bin represents increments in

mitochondrial area of 0.1 μm^2 from left to right. Range is 0 to 2 μm^2. (f) No significant difference was observed in median mitochondrial area. (g) Representative transmission electron microscopy images. Mitochondria become more rounded in moderate RV hypertrophy and more irregular in shape in RV failure, with a loss of defined cristae structure. Scale bars are 2 μm. N=3/group. Mod – moderate; Sev – severe; mtDNA – mitochondrial DNA; RV – right ventricle; RVF – right ventricular failure. Data are presented as mean±SEM. *$p<0.05$.

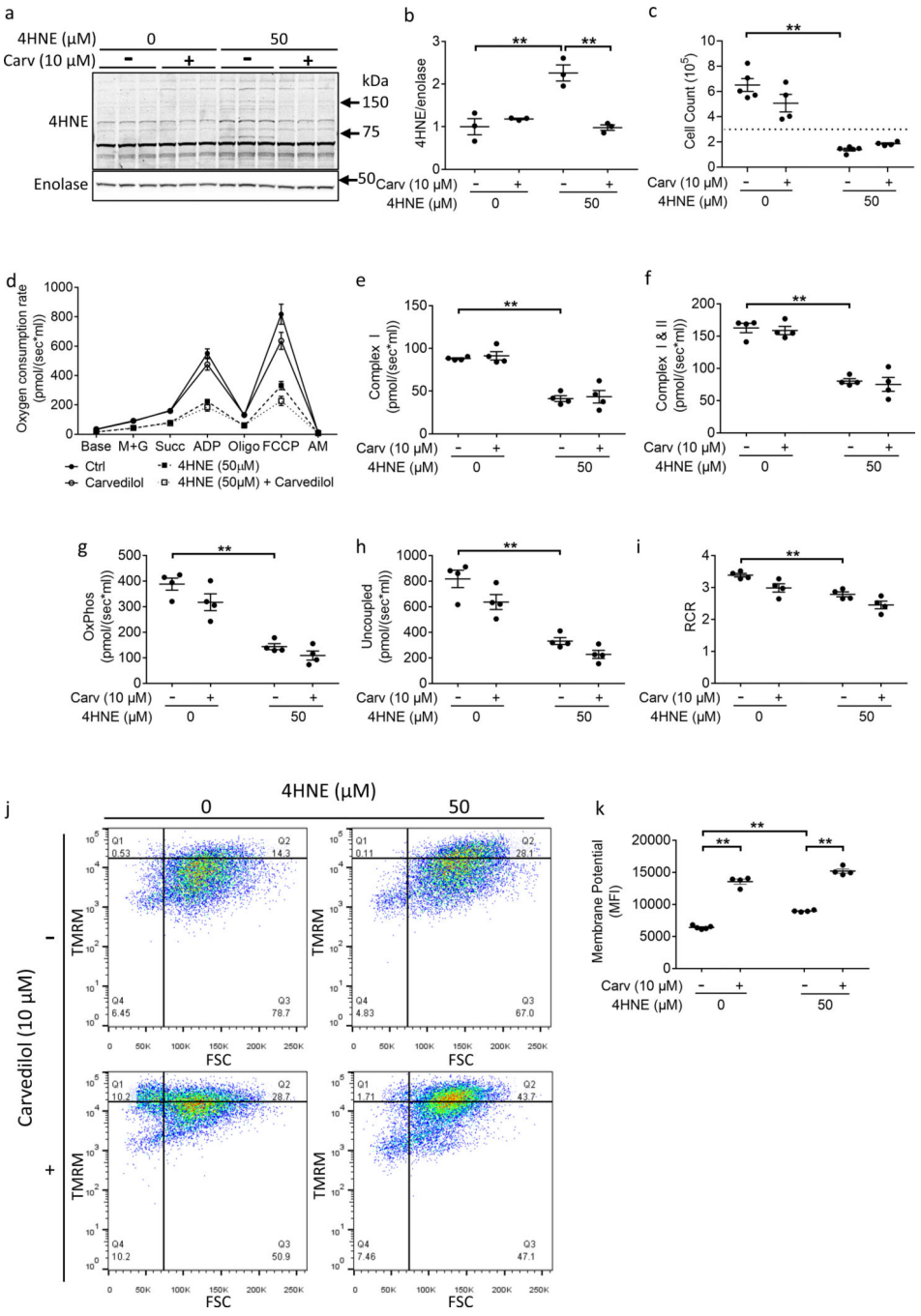

Figure 4.

4HNE treatment decreases ATP synthesis but increases mitochondrial membrane potential. HL1 Cardiomyocytes were treated with 50 μM 4HNE for 24 hours and rescue was assessed with 10 μM carvedilol. (a, b) 4HNE adducts increased following 4HNE treatment. Carvedilol decreased 4HNE adducts(N=3/group). (c) 4HNE decreased cell count - the horizontal dotted line denotes the original number of plated cells (N=4–5/group). (d-i) Oxygen consumption was assessed in response to 4HNE using high resolution respirometry. (d) Summary of the oxygen consumption data. 4HNE decreased (e, f) leak respiration, (g)

oxidative phosphorylation, (h) uncoupled respiration, and (i) respiratory control ratio (N=4/group). (j, k) However, 4HNE increased mitochondrial membrane potential, which further increased with carvedilol treatment (N=4–5/group). Carv - carvedilol; 4HNE - 4-hydroxynonenal; M+G - malate and glutamate; Succ - succinate; Oligo-oligomycin; FCCP - carbonyl cyanide 4-(trifluoromethoxy) phenylhydrazone; AM - antimycin; OxPhos - oxidative phosphorylation; RCR – respiratory control ratio; TMRM - tetramethylrhodamine, methyl ester; FSC – forward scatter; MFI – median fluorescence intensity. Data are presented as mean±SEM. **p<0.01.

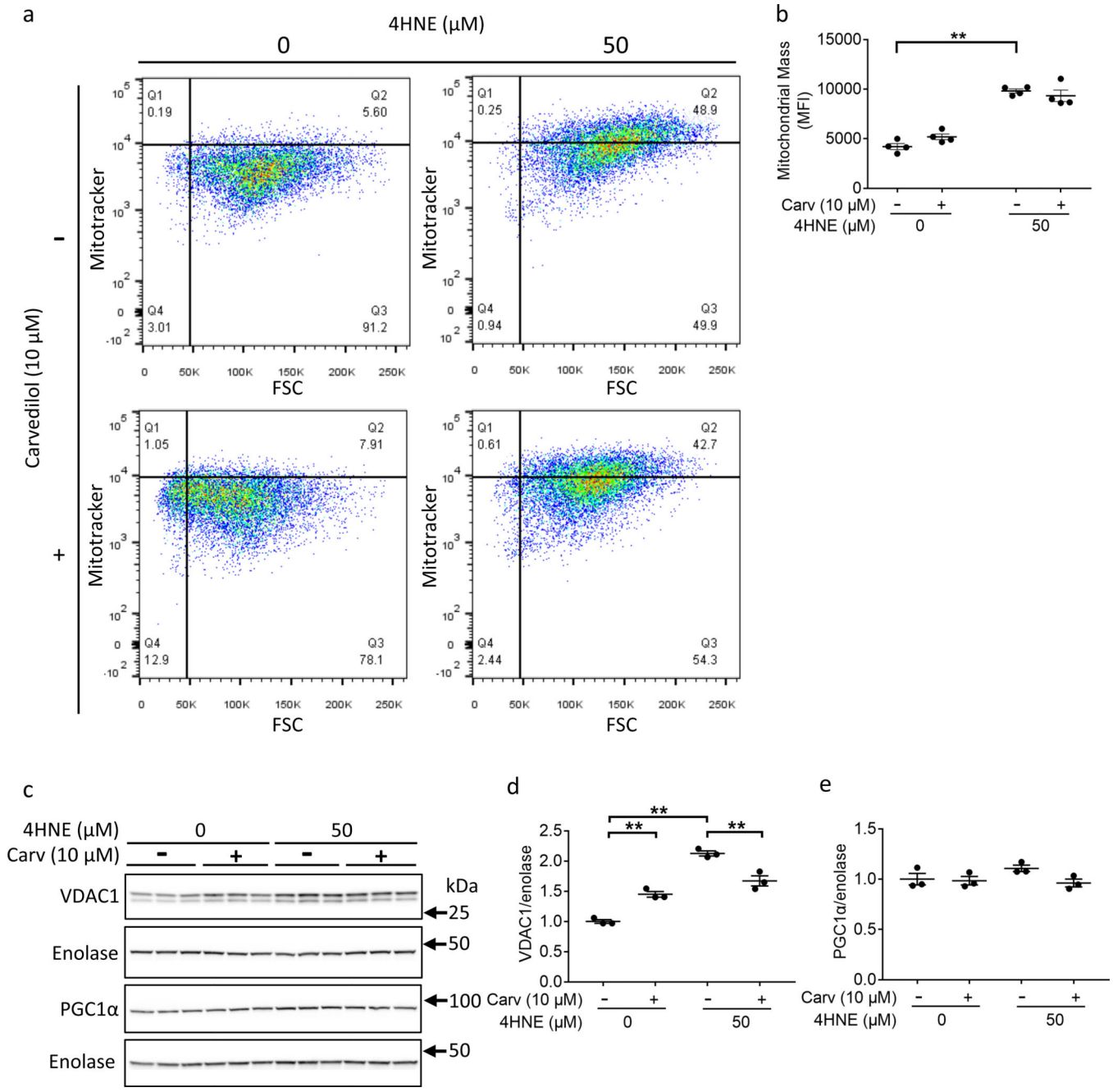

Figure 5.

4HNE treatment increases mitochondrial mass. HL1 Cardiomyocytes were treated with 50 μM 4HNE and/or 10 μM carvedilol. (a, b) 4HNE increased flow cytometric signal of Mitotracker Red CMXRos, a measure of mitochondrial mass (N=4/group). (c, d) 4HNE increased VDAC1 expression, another marker of mitochondrial mass, but this was inhibited by carvedilol. (e) 4HNE did not decrease PGC1α expression, a marker of mitochondrial biogenesis (N=3/group). 4HNE - 4-hydroxynonenal; Carv – carvedilol; FSC – forward scatter. Data are presented as mean±SEM. **p<0.01.

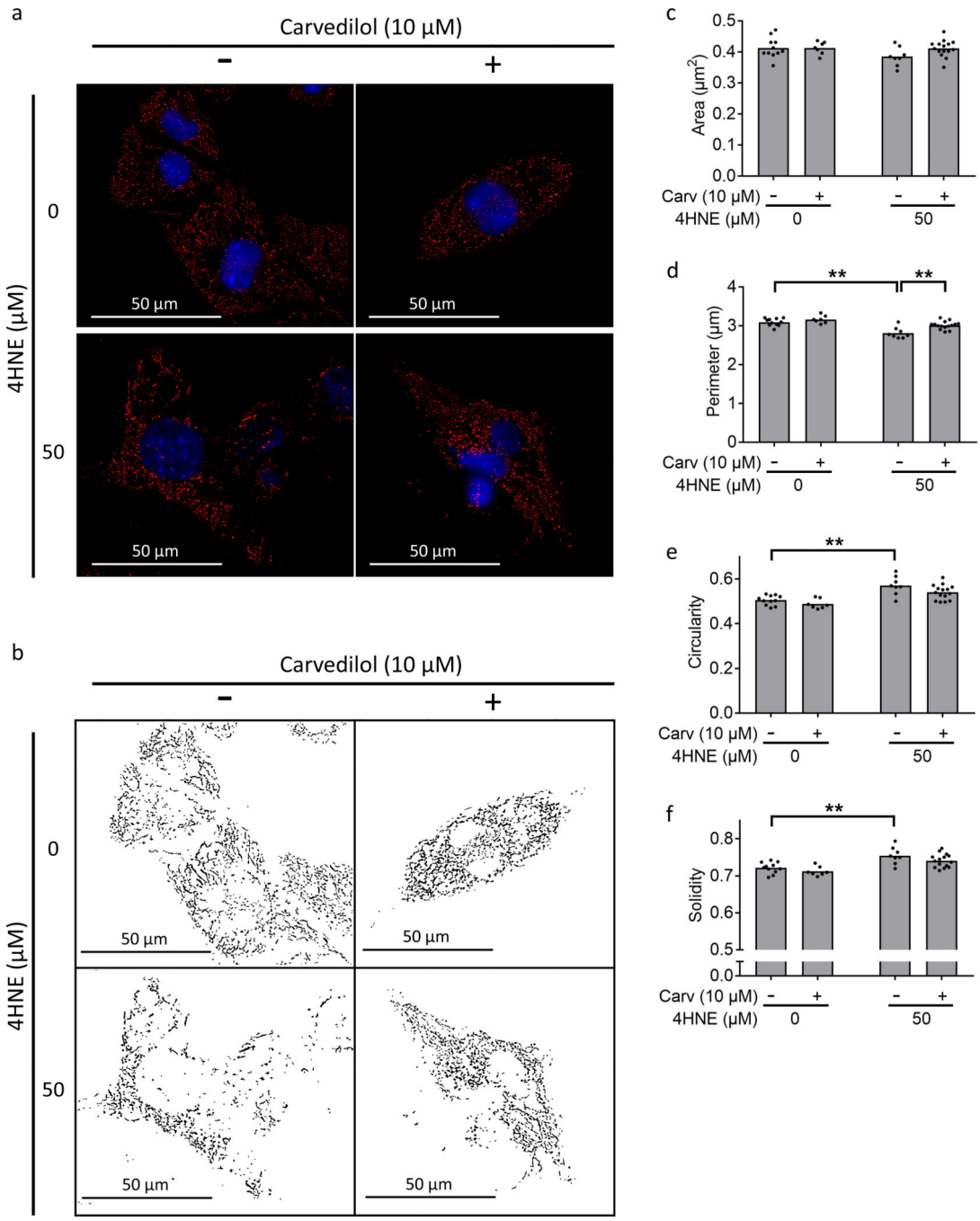

Figure 6.

4HNE decreases mitochondrial network connectivity. Cardiomyocytes were stained with Mitotracker Red CMXRos (red) and Hoechst 33342 (blue) for mitochondrial and nuclear staining, respectively. 50 μM 4HNE treatment for 24 hours (a, b) disrupted mitochondrial network connectivity and Carvedilol improved network connectivity, (c) did not demonstrate a change in mitochondrial area, (d) decreased perimeter, (e, f) increased circularity and

solidity. Scale bars are 50 μm. 4HNE - 4-hydroxynonenal. Data are presented as mean ±SEM. **p<0.01.

Table 1.

Patient Characteristics.

	Mild RV Hypertrophy	Moderate RV Hypertrophy	Severe RV Hypertrophy	RV Failure
Number of patients	3	10	3	5
Age (years)	11.3 ± 16.1	2.8 ± 4.3	25.2 ± 13.8	10.9 ± 6.9
Sex (Male)	33%	50%	33.3%	60%
Diagnoses	PS, VSD/DCRV	TOF, PS, VSD/DCRV	TOF, VSD/DCRV	AVSD, Shone's complex with PHTN
Surgical Procedure	RVOT muscle bundle resection	RVOT muscle bundle resection	RVOT muscle bundle resection	Heart transplant
Peak RVOT gradient (mmHg)	57.7 ± 2.5	82.1 ± 18.8	119.3 ± 19.1	51.8 ± 32.2
RV fractional area change (%)	46 ± 6.24	49.7 ± 7.67	43 ± 6.08	26.6 ± 3.13
Left Ventricular Ejection Fraction (%)	60 ± 6.76	62 ± 8.22	69 ± 7.45	58 ± 13.86
Medications	-	-	-	Epinephrine, Dopamine, Milrinone

Right ventricular tissue was collected at the time of surgical repair from patients with mild, moderate and severe RV hypertrophy and at the time of heart transplantation from patients with RV failure secondary to congenital heart disease. All patients with mild, moderate and severe hypertrophy had RV pressure overload with preserved systolic function. Patients with RV pressure overload with RV failure had decreased systolic function and were on systemic inotropic therapy. RV – right ventricle; RVOT – right ventricular outflow tract; PS – pulmonary stenosis; VSD – ventricular septal defect; DCRV – double chambered right ventricle; TOF – tetralogy of Fallot; AVSD – atrioventricular septal defect; PHTN – pulmonary hypertension. Data are presented as mean±SD.

Table 2.

4HNE modification of metabolic and mitochondrial proteins characterize oxidant stress in RV failure.

Category	Spot Number	4HNE-Modified Protein Name	Accession No.	Fold Change
Metabolism	22	NADH dehydrogenase [ubiquinone] iron-sulfur protein 3, mitochondrial	NDUS3_HUMAN	2.58
	11	NADH dehydrogenase [ubiquinone] iron-sulfur protein 2, mitochondrial	NDUS2_HUMAN	2.55
	12	Elongation factor Tu, mitochondrial	EFTU_HUMAN	2.53
	14	Beta-enolase	ENOB_HUMAN	2.35
	8	Dihydrolipoyl dehydrogenase, mitochondrial	DLDH_HUMAN	2.26
	16	Creatine kinase M-type	KCRM_HUMAN	2.05
	19	Malate dehydrogenase, cytoplasmic	MDHC_HUMAN	2.02
	10	Alpha-enolase	ENOA_HUMAN	1.99
	23	ES1 protein homolog, mitochondrial	ES1_HUMAN	1.88
	13	Fumarate hydratase, mitochondrial	FUMH_HUMAN	1.70
	18	Glyceraldehyde-3-phosphate dehydrogenase	G3P_HUMAN	1.69
	15	Creatine kinase S-type, mitochondrial	KCRS_HUMAN	1.68
	9	Cytochrome b-c1 complex subunit 1, mitochondrial	QCR1_HUMAN	1.66
	5	Aconitate hydratase, mitochondrial	ACON_HUMAN	1.62
	17	NADH dehydrogenase [ubiquinone] 1 alpha subcomplex subunit 10, mitochondrial	NDUAA_HUMAN	1.62
	21	Cytochrome c1, heme protein, mitochondrial	CY1_HUMAN	1.30
Structure	25	Cysteine and glycine-rich protein 3	CSRP3_HUMAN	25.64
	1	Collagen alpha-1(VI) chain	CO6A1_HUMAN	6.43
	7	Desmin	DESM_HUMAN	2.81
	6	Tubulin beta-4B chain	TBB4B_HUMAN	2.25
	2	Myosin Heavy Chain-7	MYH7_HUMAN	1.72
Survival	3	Stress-70 protein, mitochondrial	GRP75_HUMAN	3.48
	24	Superoxide dismutase [Mn], mitochondrial	SODM_HUMAN	1.96
Others	4	Serum albumin	ALBU_HUMAN	3.38
	26	Myoglobin	MYG_HUMAN	3.15
	20	Four and a half LIM domains protein 2	FHL2_HUMAN	1.85
	27	Myoglobin	MYG_HUMAN	1.45

Proteins with increased levels of 4HNE modification detected in RV failure vs. RV hypertrophy by 2D-gel electrophoresis and western blot were identified using mass spectrometry (N=1/group). 27 proteins were increased in RV failure vs. RV hypertrophy with 100% protein score confidence intervals for all proteins (>95% is considered significant). Fold change represents the increase in RV failure vs. RV hypertrophy. 4HNE - 4-Hydroxynonenal.